# SINGLE-WALLED CARBON NANOTUBES, CARBON NANOFIBERS AND LASER-INDUCED INCANDESCENCE

Randy L. Vander Wal[1], Thomas M.Ticich[2], Gordon M. Berger[1],
and Premal D. Patel[1]
[1]*National Center for Microgravity Research, NASA Glenn Research Center*
*Cleveland, OH 44135*
[2]*Centenary College, Department of Chemistry*
*Shreveport, LA 77134*

## Introduction

Many reacting flows are aerosols composed of multiple elements. Such is the case for catalyzed aerosols whose products will be chemically and physically different than the catalyst particle. One of the most sought aerosols is carbon nanotubes (CNTs). Aerosol synthesis of CNTs is currently the method of choice for both purity and yield of CNTs and offers the opportunity for both continuous processing and scalability. Catalyzed by metal nanoparticles in hydrocarbon or CO gas mixtures at elevated temperatures, these nanostructures are comprised mainly of elemental carbon. Depending upon the structural details of the catalyst particle, the nanotube morphology will vary between single-walled nanotubes (SWNTs), multi-walled nanotubes (MWNTs) and nanofibers. Currently, yield measurements and synthesis conditions are characterized by collecting samples for subsequent processing and electron microscope analysis, steps which do not provide real-time feedback. Clearly, process control and optimization of nanotube/nanofiber production could benefit from a real time, in situ diagnostic. One such potential diagnostic is laser-induced incandescence (LII).

LII has been widely tested and used for measurement of carbonaceous aerosols in reacting flows [2]. LII has been applied to soot measurements within a wide variety of combustion systems including simple laboratory scale diffusion and premixed flames [3-8], in situ engine measurements [9], and aircraft engine exhaust [10]. The foundational principle of LII is the use of pulsed laser heating to elevate the temperature of the irradiated soot to temperatures near the vaporization temperature of carbon, far above that of the ambient flame gases and the surrounding particulate matter. Consequently, the spectral emission is both dramatically increased and blue-shifted relative to the non-laser heated soot and flame gases. Through selective spectral and temporal detection, this incandescence emission may be detected apart from the non-laser heated soot and flame gases and quantified for absolute soot volume fraction determination [2,11].

Successful implementation of LII relies upon judicious choice of excitation and detection conditions [11-13]. Excitation conditions encompass choice of excitation wavelength and laser fluence. Detection conditions include choice of detection wavelength, spectral bandpass about the central wavelength and detection delay and duration relative to the excitation laser pulse usually corresponding to the peak of the signal intensity. Though

many of these issues have been addressed for LII applied to soot, a homogeneous aerosol consisting mainly of carbon, metal catalyzed carbon nanotubes and nanofibers are physically and chemically heterogeneous.

## Specific Objectives

Application of LII to a chemically and physically heterogeneous aerosol, such as carbon nanotubes or nanofibers brings forth several questions.
Questions include:

1. Does the metal nanoparticle catalyzing the carbon nanotube or nanofiber also simultaneously incandesce? Can this even be determined?
2. If the particle does incandesce, can this emission be detected separately from that arising from the laser-heated carbon nanostructure as a measure of the metal particle concentration?
3. Will vaporization wipe out incandescence from SWNTs, because there is no solid material left to incandesce?
4. Can the laser initiate reactions between the catalyst metal particles and the carbon?
5. Does the incandescence scale with the mass fraction of aerosol? Can this be validated against an independent technique?

Despite this range of possibilities, it is expected that some questions could be answered by impact on the spectral and/or temporal evolution of the LII signal. For example, incandescence from metal nanoparticles ought to be readily recognizable by the appearance of structured emission and the different decay rate of such emission relative to that from the near blackbody emission of the carbon nanotube or nanofiber [14]. Emission from electronically excited vaporized material ought to be identifiable by its distinctly different spectral and temporal evolution compared to incandescence. The onset of vaporization ought to be identifiable from fluence dependence measurements. The vaporization effect(s) upon the emission signal ought to be identifiable by the variation of the signal temporal evolution with laser fluence. Emission arising from condensed phase reaction products (whose synthesis was initiated by the pulsed laser heating) ought to again produce distinctly different spectral and temporal emission relative to that from unreacted material [15], namely the portion of the carbon nanotube that would be uninfluenced by the catalyst particle.

Thus to examine the viability of LII for measuring these aerosols, we investigated the capability of LII applied to CNTs within a reacting flow. The work presented here characterizes LII applied to CNTs within a flame environment.

## Experimental

Light at 1064 nm, generated by a Nd:YAG laser, was directed to pass through the flame between two steel chimneys, 1 inch O.D. and 3 inches long. A 1/4 inch diameter aperture through a 1/16 inch thick steel disk trimmed the beam spatial intensity profile to approximate a top-hat profile within the near field.

LII was collected by a quartz optical fiber bundle. A commercial quartz lens assembly was placed on the fiber to accommodate the fiber's numerical aperture. A second telescope served to relay the laser beam image onto the commercial lens. The relay telescope was formed by two quartz lenses, each 50.5 mm diameter, with 100 and 250 mm focal lengths. The other end of the fiber bundle terminated in a rectangular geometry matching the entrance slit for the spectrograph or spectrometer. An intensified cooled CCD, under computer control, captured spectra at selected times relative to the excitation laser pulse. The pulser for the camera intensifier was synchronized to the laser by a digital delay generator. Spectral resolution was determined by the entrance slit and was found to be 5 nm by comparison to Hg lamp spectral emission lines. Spectral wavelength calibration was achieved by comparison to tabulated Hg emission lines.

A PMT attached to a spectrometer detected the temporal emission of the LII at selected wavelengths. Operated at 900 V, the PMT temporal resolution was judged to be approximately 2 ns. The temporal evolution data was captured by a digitizing oscilloscope with GHz bandwidth. Spectral and temporal data was processed using commercial software.

Single-walled nanotubes and nanofibers were synthesized within a pyrolysis flame configuration. Nebulization of an ethanol solution of iron nitrate or nickel nitrate at a concentration of 6mg/ml produced an aerosol of metal nitrate particles. This mist was entrained using a mixture of CO, H2 and He, (0.25 SLPM for each gas) for the iron solution or C2H2, H2 and CO (0.1, 0.5, 0.5 SLPM) for the Ni solution. These gas mixtures yielded nearly exclusively SWNTs with Fe nanoparticles and nanofibers with Ni particles. Further details of the tested gas mixtures, solution concentrations and solvent effects are reported elsewhere [16,17]. The aerosol and reactive gas mixture formed the fuel for the pyrolysis flame.

## Background

Metal catalyzed SWNTs and nanofibers represent a unique measurement challenge to optical diagnostics. First, the aerosol to be measured is composed of two elements in intimate association. Additionally, each of these may exist in a variety of forms. In the case of SWNTs, as Fig. 1 shows, numerous Fe nanoparticles are distributed along the nanotube walls. Though difficult to observe, many are likely at the tips of the nanotubes as suggested by the yarmulke formation mechanism [18]. In contrast, for the Ni catalyzed nanofibers, Ni nanoparticles are clearly observed at the ends of the nanofibers. Isolated Ni nanoparticles are generally not observed. As shown in Fig. 1, these catalyst nanoparticles are partially covered by or contained within the nanofiber. Finally, the Ni particles are much larger than the Fe nanoparticles.

**Fe Catalyzed SWNTs** **Ni catalyzed nanofibers**

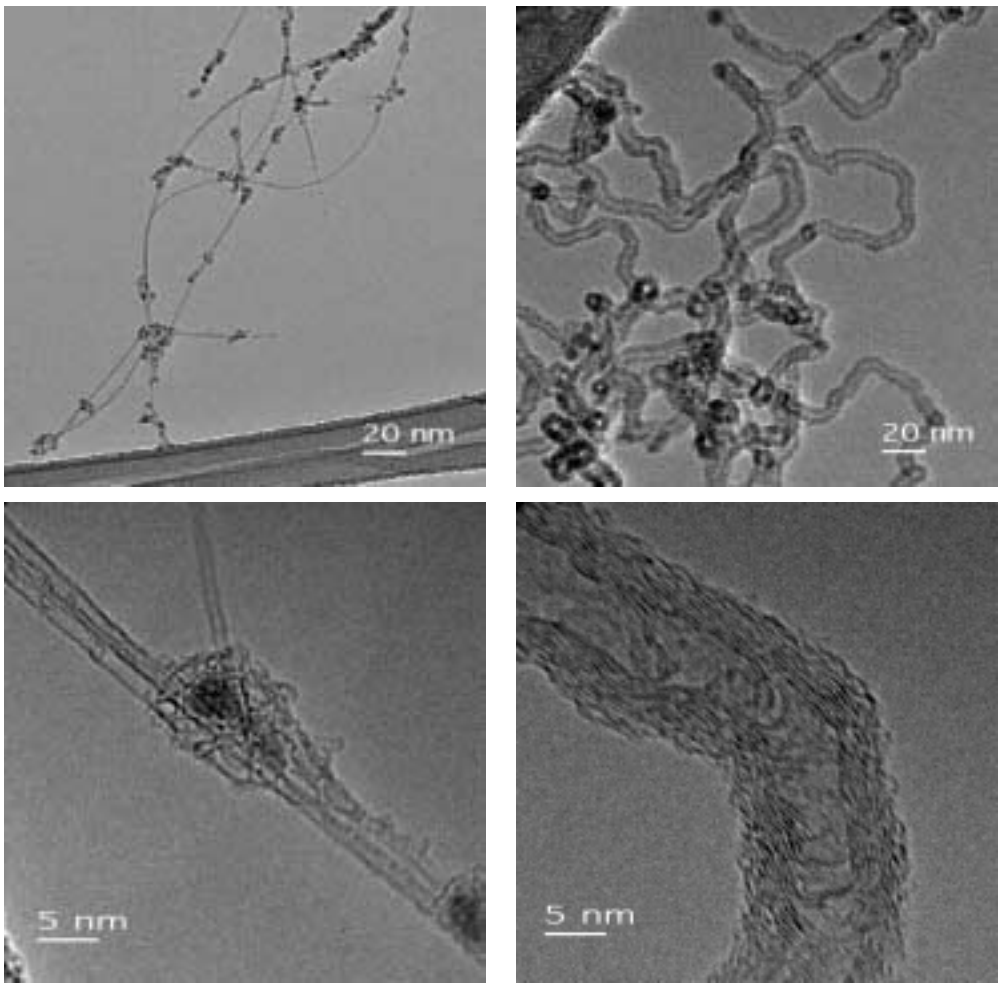


Figure 1. HRTEM images of Fe catalyzed SWNTs and Ni catalyzed nanofibers collected from the pyrolysis flame. The images show the material as sampled directly from the flame, without purification or processing.

The carbon nanostructures are also different sizes, as seen by comparison of the SWNTs in Fig. 1 and the nanofibers in Fig. 1. As illustrated by the HRTEM images in Fig. 1, the structure of the SWNTs is that of a single atomic layer of carbon, forming a hollow cylinder. SWNTs are, however, frequently found as bundles or ropes consisting of a few to several nanotubes that are physically not chemically bound together [18]. Hence, these nanostructures possess widely varying aspect ratios. In contrast to the SWNT, nanofibers are comprised of stacked graphene segments. As seen in Fig. 1, the nanofibers may possess a variety of morphologies depending upon the length and orientation of the graphene segments with respect to the filament axis.

These structures are formed via a different growth process involving carbon solvation into, diffusion through and precipitation from the catalyst particle [19]. As a dual element

system with each element in different forms and exhibiting varying “phases” or levels of organization, such as graphitic quality; widely different signals could be expected. Moreover, the intimate “attachment” of the catalyst particles to the catalyzed carbon nanostructures introduces further possible complications related to reactions between the metal nanoparticle and carbon upon pulsed laser heating, as discussed previously.

## Results and Discussion

### Spectrally Resolved Emission

As a starting point for identifying suitable spectral regions for detection of incandescence and spectral interferences, temporally resolved emission spectra were obtained. These were collected at the highest available laser fluence, 0.8 J/cm$^2$ to best detect possible spectral interferences from vaporized species.

In comparison to LII spectra obtained on metal aerosols [14], there is absence of structured emission in the spectra shown in Fig. 2. This suggests an absence of electronically excited atoms or molecules produced by the pulsed laser heating. Similar results have been attained with LII applied to soot, when using 1064 nm excitation [3,12]. This apparent absence of Fe or Ni and atomic, molecular or small cluster emission potentially offers straightforward interpretation of the emission as arising from SWNTs and nanofibers.

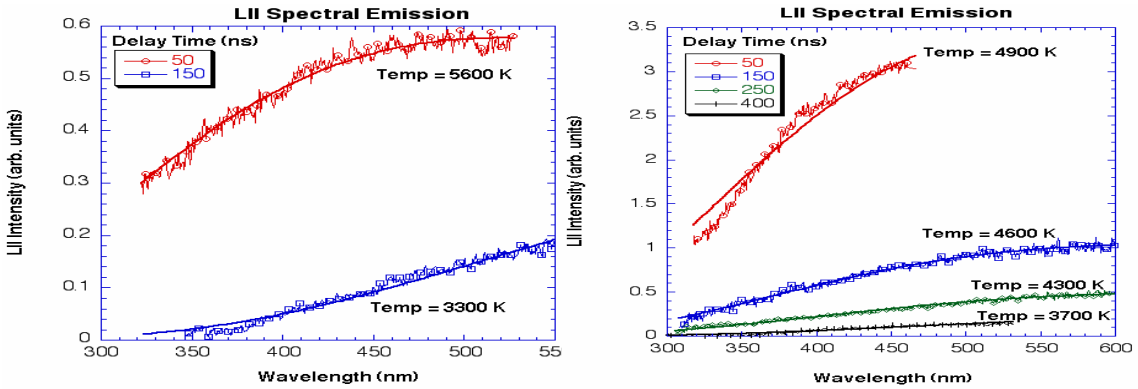


Figure 2. Spectrally resolved emission signals collected at the indicated times after the excitation laser pulse. The blackbody curve fits are the solid lines.

Yet these spectra differ substantially from blackbody emission characteristic of a carbonaceous aerosol. As shown for both the Fe and Ni pyrolysis flames, the fitted temperatures of the initial spectra are substantially higher than those associated with the vaporization temperature of carbon, roughly 4000 K. It should be noted that carbon has the highest vaporization temperature of the materials within the flame environment used here. Only ionic, atomic and molecular emission can create such apparent elevated temperatures, not a superheated, solid nanostructure. These species likely exist within a laser vaporized plasma. With increasing time after the excitation laser pulse, the spectra become consistent with blackbody emission commensurate with

"solid" carbon material (i.e. < 4000 K). Collisional quenching and radiative cooling of electronically excited species will occur at a far faster rate than conductive cooling of a solid nanostructure [20]. Essentially, spectra collected at times delayed after the excitation laser pulse allow for plasma dissipation processes after which only incandescence becomes detectable.

## Temporally Resolved Emission

In order to clarify/identify the origins of the wavelength resolved emission spectra, temporally resolved signals were collected at fixed detection wavelengths of 300, 450 and 600 nm. The same value of laser fluence, 0.8 J/cm$^2$ as used for the temporally resolved emission spectra generated these signals. These data are plotted in Fig. 3 for both the Fe and Ni pyrolysis flames. The signal intensities have been scaled to a common peak intensity in order to examine differences in the temporal decays. As shown, for both the Fe and Ni based systems, there is little variation in the temporal decay with increasing detection wavelength. Moreover, for any given detection wavelength, there is little difference in the decay rate between the Fe and Ni systems, despite the quite different sizes for the catalyst particles and carbon nanostructures between these two systems, as shown in Fig. 1.

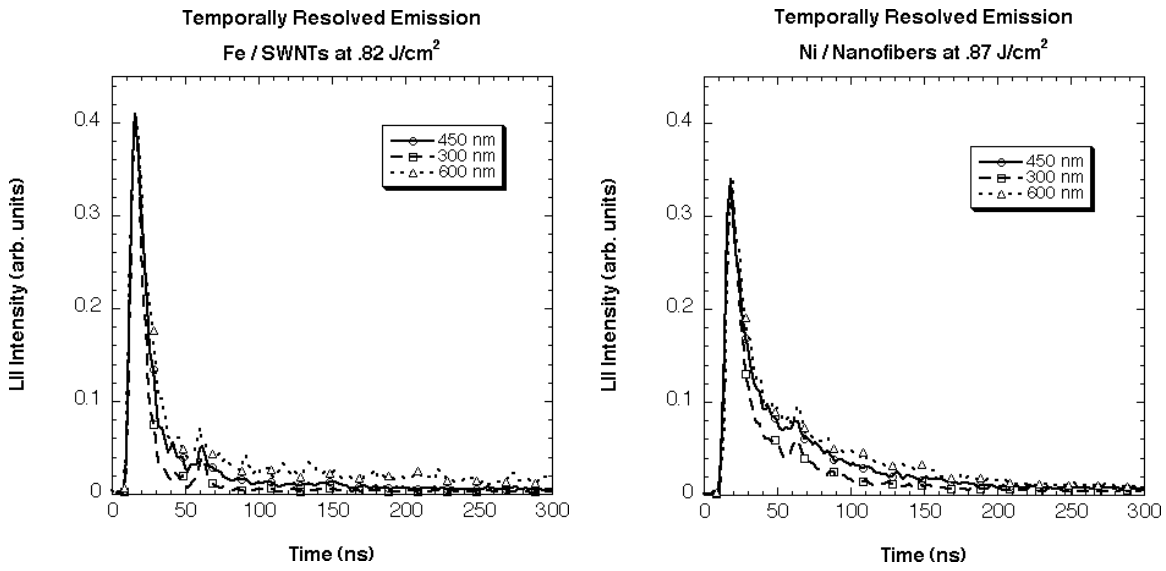


Figure 3. Temporally resolved emission signals collected at the nominal indicated wavelengths for the Fe and Ni based pyrolysis flame systems.

Variation in the time evolution at these different wavelengths can reveal contributions to the observed laser induced emission in addition to incandescence from the laser heated nanostructures. If only blackbody radiation were contributing to the signal, a more significant decrease in the temporal decay rate would be expected with increasing detection wavelength. That such behavior is not observed indicates a different origin of the emission. The close similarity in the emission decay rates between the Fe and Ni

systems indicates vaporization producing a super-heated plasma, producing a "blackbody" continuum emission. Under severe vaporization, if any solid material remains to incandesce at longer times, [13,15], its contribution to the detected radiation will be small. The solid material may arise either from condensation of plasma species or material heated by the wings of the near top-hat beam profile.

## Fluence Dependencies

Having determined that vaporization occurs at these fluences, leaving little or no material from either SWNT or nanofibers, we collected fluence dependence data. Fluence dependencies serve as a starting point for determining the onset of vaporization and its contribution to the observed signal. The data shown in Fig. 4 were generated using a "prompt" signal collection gate, beginning with the peak LII intensity, for the indicated signal integration times following the laser pulse as indicated in the Figure. As seen in Fig. 4, for both the Fe and Ni systems, the signal increases, reaches a near maximum and then decreases. Traditionally, the decrease has been attributed to laser induced vaporization resulting in mass loss leaving less material to incandesce subsequent to the laser pulse [5,13,15]. The point of decreasing signal has been referred to as the vaporization threshold.

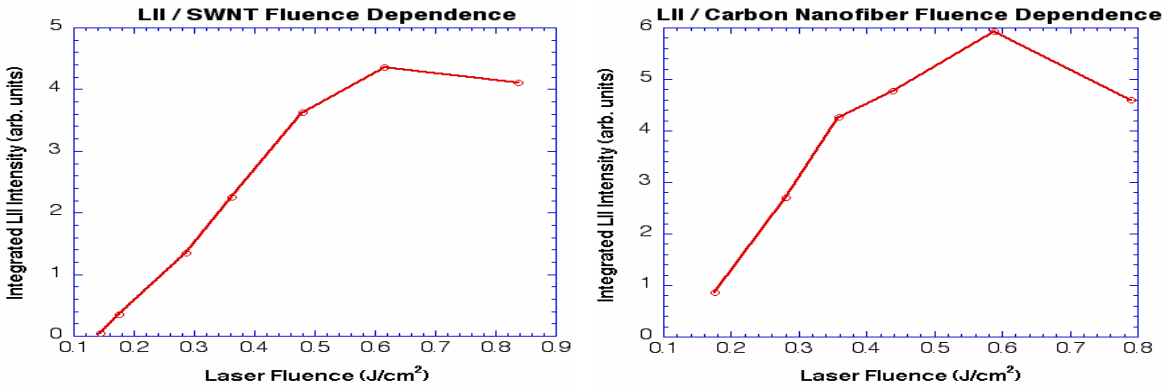


Figure 4. Fluence dependencies for the Fe and Ni based pyrolysis flame systems. For each curve, a prompt detection gate of 50 ns duration, coincident with the end of the excitation laser pulse.

## Two Laser Pulse Measurements

Two-laser pulse measurements are used to further probe the effects of laser induced changes upon the optical signal. Two-laser pulse experiments reveal that other material changes are produced at fluence below the apparent vaporization threshold, leading to nanostructures with different optical and thermal properties. Results from these measurements will be conveyed during the presentation.

## Conclusions

In conclusion, it is likely, based on previous studies of LII applied to metal aerosols, that the catalyst particles contribute to the incandescence and/or plasma emission, the particular process depending upon the laser fluence. The super-elevated temperatures,

derived from blackbody fits to spectrally resolved emission, observed using laser fluences of 0.8 J/cm$^2$, suggest continuum emission from a laser generated plasma. The absence of atomic, molecular and cluster electronic emission upon the “blackbody” (plasma) radiation is surprising, but highlights the utility of 1064 nm excitation in order to avoid electronic excitation of plasma species.

Unlike previous observations, LII from the metal nanoparticles does not produce distinct spectral signatures. Thus, their relative contribution to the emission signal is not readily extracted from that arising from the carbon nanotubes or nanofibers. Additionally, it is not readily rejected, spectrally nor temporally. The short temporal existence of the emission signal from Fe-SWNT system and Ni-nanofiber system confirms that vaporization occurs at high laser fluences, e.g. 0.8 J/cm$^2$. In this case there is no remaining solid incandescence. Fluence dependencies reveal the onset of laser induced vaporization as commensurate with that of pure carbonaceous material, approximately 0.6 J/cm$^2$.

## Acknowledgements

This work was supported by a NASA NRA 97-HEDs-01 combustion award (RVW), and a Director’s Strategic Research Fund, administered through NASA cooperative agreement NCC3-975 with The National Center for Microgravity Research on Fluids and Combustion (NCMR) at NASA Glenn Research Center. The authors thank David R. Hull for the HRTEM imaging.

## References

[1] Collins PG, Avouris P. Scientific American, Dec. 2000; 38-45.
[2] Eckbreth AC. “Laser diagnostics for combustion temperature and species”, Gordon and Breach, 2nd Ed., 1996.
[3] Vander Wal RL, Weiland KJ. Appl. Phys. 1994; B59:445-452.
[4] Quay B, Lee TW, Ni T, and Santoro RJ, Combust. and Flame 1994; 97:384-392.
[5] Shaddix C, Smyth K. Combust. and Flame 1996; 107:418-452.
[6] McManus KR, Frank J, Allen MG, Rawlins WT. 1998; AIAA Paper 98-0159.
[7] De Croix MW, Roberts WL. Combust. Sci. and Technol. 1999; 146:57-84.
[8] Walsh KT, Fielding J, Smooke MD, Long MB. The Twenty-Eighth Symposium (International) on Combustion, The Combustion Institute, Pittsburgh, PA 2000; 1973-1984.
[9] Zhao H, Ladommatos N. Prog. Energy Combust. Sci. 1998; 24:221-255.
[10] Black JD. SPIE Vol. 3821, 1999; 209-215.
[11] Vander Wal RL. Contractor Report, NASA/CR—1997-206325.
[12] Vander Wal RL. Appl. Opt. 1996; 35:6548-6559.
[13] Vander Wal RL, Jensen, KA. Appl. Opt. 1998; 37:1607-1616.
[14] Vander Wal RL, Ticich TM, West J. Jr. Appl. Opt. 1999; 38: 5867-5879.
[15] Vander Wal RL, Ticich TM, Stephens AB. Appl. Phys.1998; B67:115-123.
[16] Vander Wal RL, Hall LJ. Chem. Phys. Lett. 2001; 349:178-184.
[17] Vander Wal RL, Choi MY, Lee K.-O. Combust. and Flame 1995; 102:200-204.

[18] Dai H, Rinzler AG, Nikolaev P, Thess A, Colbert DT, Smalley RE. Chem. Phys. Lett. 1996; 260:471-475.
[19] Baker RTK, Harris PS, Thomas RB, Waite RJ. J. of Catalysis 1973; 30:86.
[20] Radziemski LJ, Cremers DA. “Laser induced plasmas and applications”, Marcel Dekker, Inc. (1989).